AD-A042 353 IRT CORP SAN DIEGO CALIF F/G 20/14
ANALYSIS AND TESTS OF A 90-CM RIGHT CIRCULAR CYLINDER IN THE PI--ETC(U)
JUN 77 R KEYSER, W D SWIFT F29601-74-C-0105
UNCLASSIFIED IRT-8114-045 AFWL-TR-77-19 NL

| OF |
ADA
042353

END

DATE
FILMED
8-77

AFWL-TR-
77-19

2

ANALYSIS AND TESTS OF A 90-cm RIGHT CIRCULAR CYLINDER IN THE PIMBS 1A PHOTO ENVIRONMENT

IRT Corporation
P.O. Box 80817
San Diego, CA 92138

June 1977

Final Report

Approved for public release; distribution unlimited.

AIR FORCE WEAPONS LABORATORY
Air Force Systems Command
Kirtland Air Force Base, NM 87117

This final report was prepared by IRT Corporation, San Diego, California, under Contract F29601-74-C-0105, Job Order 4695039 with the Air Force Weapons Laboratory, Kirtland Air Force Base, New Mexico. Mr. William D. Bell (DYC) was the Laboratory Project Officer-in-Charge.

Then US Government drawings, specifications, or other data are used for any purpose other than a definitely related Government procurement operation, the Government thereby incurs no responsibility nor any obligation whatsoever, and the fact that the Government may have formulated, furnished, or in any way supplied the said drawings, specifications, or other data, is not to be regarded by implication or otherwise, as in any manner licensing the holder or any other person or corporation, or conveying any rights or permission to manufacture, use, or sell any patented invention that may in any way be related thereto.

This report has been reviewed by the Information Office (OI) and is releasable to the National Technical Information Service (NTIS). At NTIS, it will be available to the general public, including foreign nations.

This technical report has been reviewed and is approved for publication.

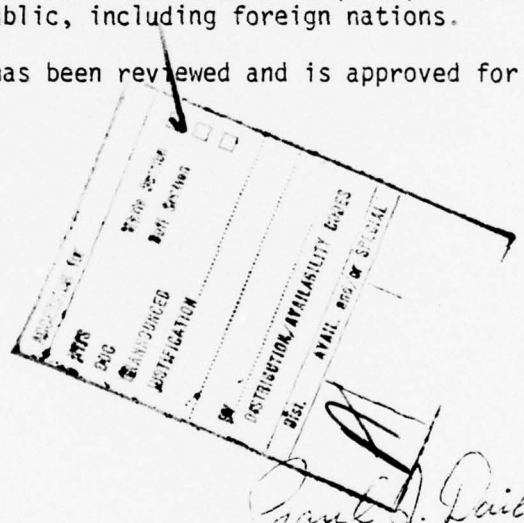

William D Bell
WILLIAM D. BELL
Project Officer

Miles T Barnett
MILES T. BARNETT
Major, USAF
Chief, Satellite and C^3 Branch

Paul J. Daily
PAUL J. DAILY
Colonel, USAF
Chief, Technology and Analysis Division

DO NOT RETURN THIS COPY. RETAIN OR DESTROY.

UNCLASSIFIED

SECURITY CLASSIFICATION OF THIS PAGE (When Date Entered)

REPORT DOCUMENTATION PAGE

READ INSTRUCTIONS BEFORE COMPLETING FORM

1. REPORT NUMBER: AFWL-TR-77-19	2. GOVT ACCESSION NO.
3. RECIPIENT'S CATALOG NUMBER	
4. TITLE (and Subtitle): ANALYSIS AND TESTS OF A 90-cm RIGHT CIRCULAR CYLINDER IN THE PIMBS 1A PHOTON ENVIRONMENT.	5. TYPE OF REPORT & PERIOD COVERED: Final Report
	6. PERFORMING ORG. REPORT NUMBER: IRT-8114-045
7. AUTHOR(s): R. Keyser, W. D. Swift	8. CONTRACT OR GRANT NUMBER(s): F29601-74-C-0105
9. PERFORMING ORGANIZATION NAME AND ADDRESS: IRT Corporation, P. O. Box 80817, San Diego, CA 92138	10. PROGRAM ELEMENT, PROJECT, TASK AREA & WORK UNIT NUMBERS: 64711F, 46950309
11. CONTROLLING OFFICE NAME AND ADDRESS: Air Force Weapons Laboratory (DYC), Kirtland AFB, NM 87117	12. REPORT DATE: June 1977
	13. NUMBER OF PAGES: 28
14. MONITORING AGENCY NAME & ADDRESS (if different from Controlling Office)	15. SECURITY CLASS. (of this report): UNCLASSIFIED
	15a. DECLASSIFICATION/ DOWNGRADING SCHEDULE

16. DISTRIBUTION STATEMENT (of this Report)

Approved for public release; distribution unlimited.

17. DISTRIBUTION STATEMENT (of the abstract entered in Block 20, if different from Report)

18. SUPPLEMENTARY NOTES

19. KEY WORDS (Continue on reverse side if necessary and identify by block number)

SGEMP analysis
Analysis verification
Photon SGEMP experiments
QUICKE2
ABORC

20. ABSTRACT (Continue on reverse side if necessary and identify by block number)

An initial analysis verification experiment is described, based on a 90-cm right circular cylinder exposed to low-level, low-frequency, 75-keV bremsthrlung, x-ray source. Pretest analytical predictions of several surface H fields on the cylinder were made using QUICKE2 to calculate the electron emission from the object, for the expected photon pulse, and the 2D particle code ABORC. These were then compared to the experimental results and found

(over) → next page

DD FORM 1 JAN 73 1473 EDITION OF 1 NOV 65 IS OBSOLETE

UNCLASSIFIED

SECURITY CLASSIFICATION OF THIS PAGE (When Date Entered)

409388

ABSTRACT (cont'd)

(+2.6 or -0.7)

cont → to be higher by a factor of 2.6 $^{+0.6}_{-0.7}$. This is believed to result from emission that was a factor of about 2 lower than expected, as measured in a separate biased x-ray diode experiment.

TABLE OF CONTENTS

LIST OF ILLUSTRATIONS

SECTION I

INTRODUCTION

An initial analysis verification effort has been completed, utilizing a simple right circular cylinder as the test object. A set of pretest predictions was made for this object based on the expected PIMBS IA photon pulse characteristics, using strictly analytical tools, i.e., QUICKE2 for electron emission and the ABORC code for surface current responses. The object was then tested in the actual photon environment generated by the PIMBS IA source, and the responses measured. The reverse electron emission yield and approximate spectrum for the surface material used on the cylinder were also measured in a separate experiment, using a biased X-ray diode. This allows any disagreement between analysis and experimental results to be separated into emission and particle motion components. Comparison of the prediction and experimental responses test the ability of the codes to predict the response of this very simple geometry in a low fluence (nonspace-charge-limited), low-frequency (nonresonant) regime. This is a very low stress test of the tools, particularly ABORC.

The experiment was performed in a vacuum environment using a 4-meter diameter, 6-meter long tank. The walls of this tank form the outer boundary for the analytical predictions. The body is dc isolated from the vacuum tank.

The results of this effort are reported in the following pages. The pretest predictions are presented first. Then the experiment is described and the experimental results presented. Comparisons of the analytical and experimental results are made and conclusions drawn from these comparisons.

PRETEST PREDICTIONS

The experiment setup analyzed consisted of a 90-cm diameter by 90-cm high right circular cylinder, irradiated end on, with a source-to-object spacing of 1.4-m. The axis of the cylinder coincided with the axis of the vacuum tank so that, except for minor disturbances, the experimental configuration was axisymmetric and therefore amenable to accurate solution with the two-dimensional system generated electromagnetic pulse (2D SGEMP) codes. All surfaces were plated with 60 percent tin, 40 percent lead solder composition by weight.

Pretest predictions of the cylinder response were made using the ABORC computer code for particle pushing and QUICKE2 for emission calculations. The emission calculations with a 1/2-mil aluminum filter are shown in Figure 1. The reverse emission level is 2×10^{-6} coulomb per cal from the tin lead solder that coats the cylinder. For the expected 55-nsec wide PIMBS pulse and $\sim 1.4 \times 10^{-5}$ cal/cm^2 predicted fluence with a 1/2-mil aluminum filter, the emission current density is 5.1 A/m^2, and the current emitted from the cylinder is 3.3 amps total.

The ABORC predictions for the cylinder in the tank are shown in Figures 2 and 3 for a slightly higher emission current of 3.5 amps. Three sets of predictions are actually shown in these two figures. Figure 2 shows the predicted body currents for the case of the 1/2-mil aluminum filter over the source and for the case of a high-transparency screen filter over the source. The latter filter allows more of the low-energy photons to shine through, with a resultant higher emission current density (7.9 A/m^2). The purpose of running both cases was to determine just how much body response was lost by going to the solid filter rather than the screen. The results shown in Figure 2 are for emission from the body only. In Figure 3, emission from the tank walls has been included to determine the effect on body response of these electrons. These latter calculations divided the tank side walls into 6 different emission zones to accurately account for different fluence levels and photon arrival times. Including tank emission results in an approximately 10 to 20 percent increase in the cylinder surface H fields.

The results of the ABORC predictions are summarized in Table 1 in terms of peak H fields and the expected signal in the CML 6 $\dot{B}$ probes. The $\dot{B}$ signals were estimated by several different methods, which gave a maximum spread of

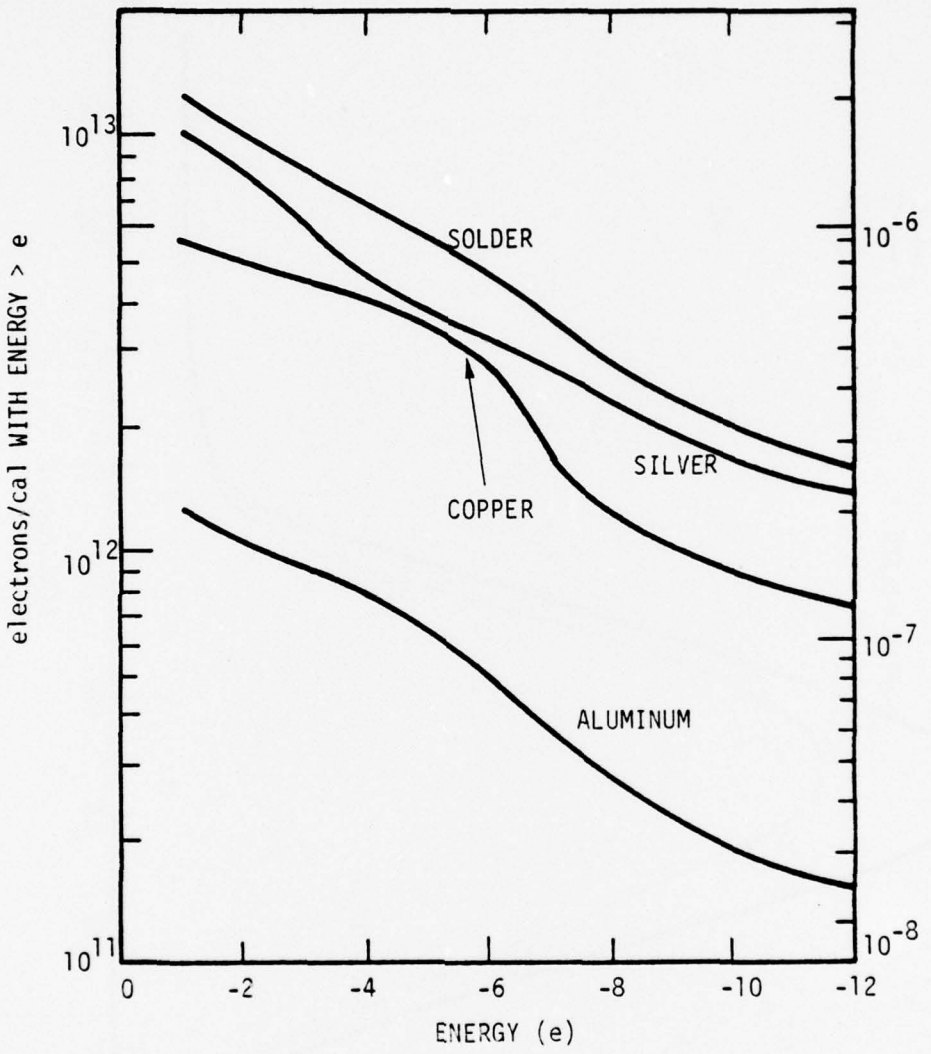

Figure 1. Reverse emission of 75-kV bremsstrahlung for PIMBS IA through 1/2-mil aluminum foil--QUICKE2 predictions

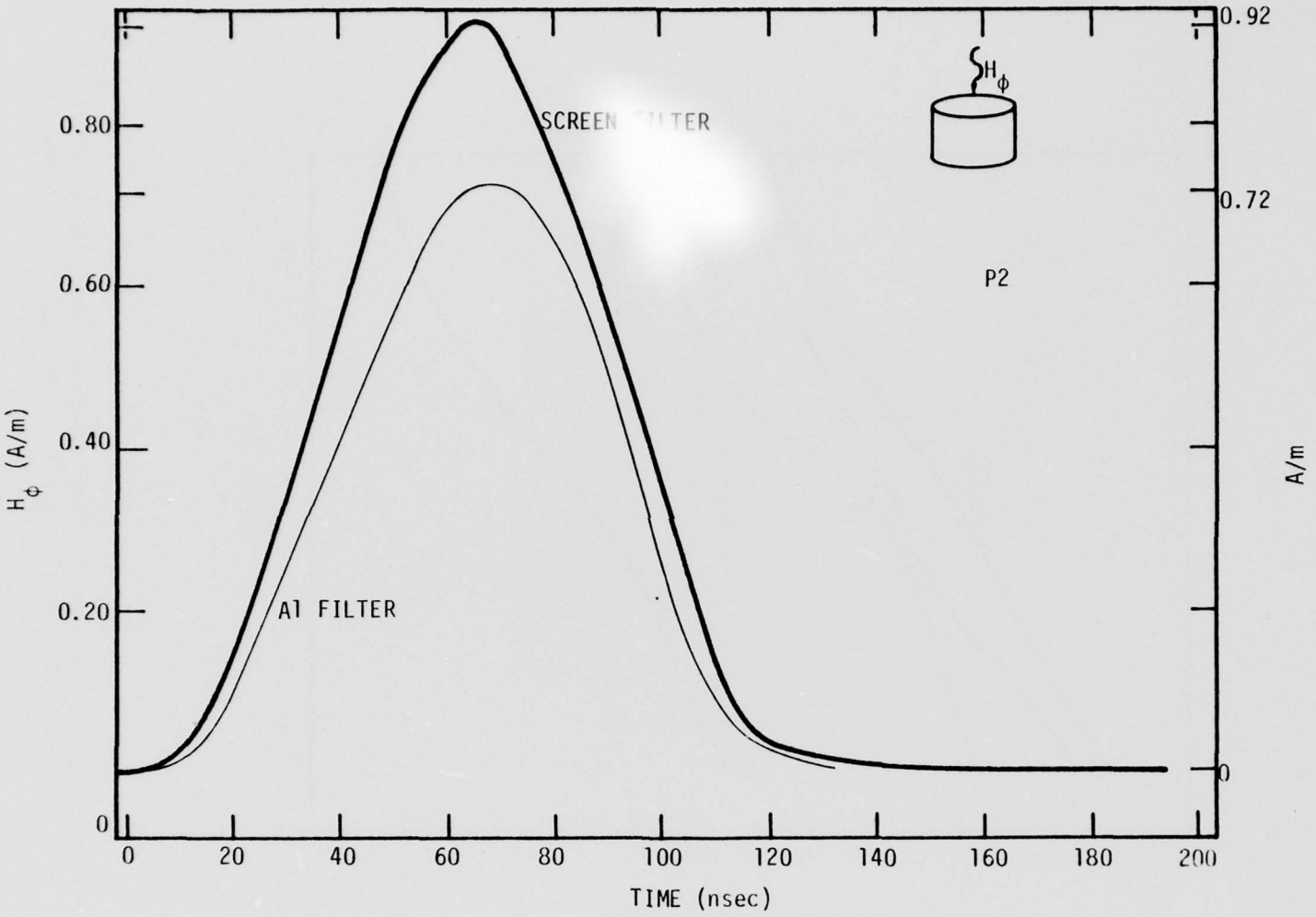

Figure 2. ABORC prediction of body response: 1/2-mil Al filter and high transparency screen, emission from body only

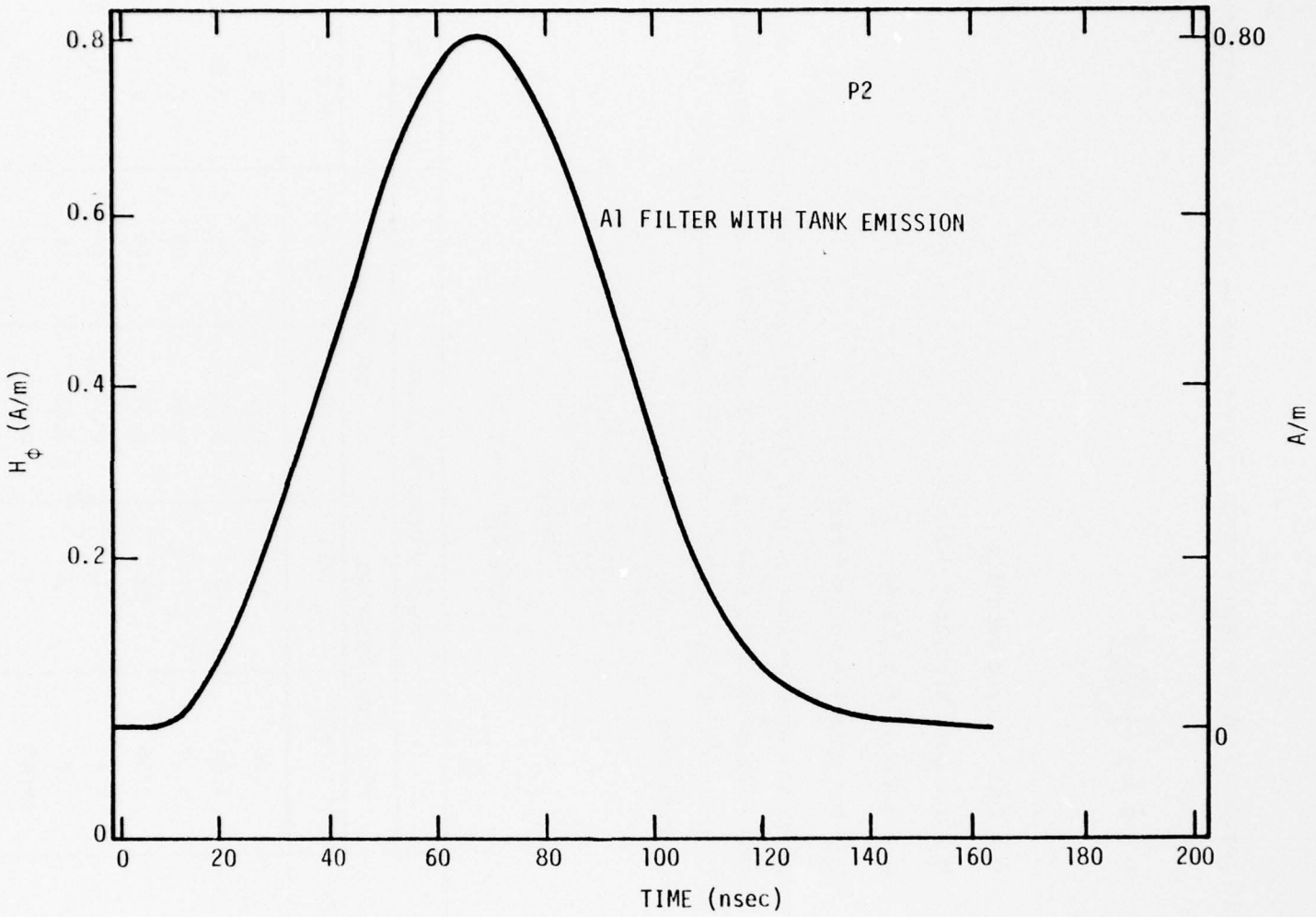

Figure 3. ABORC prediction of body response: 1/2-mil Al filter, emission from body and tank

about ±10 percent from the values shown. The values in Table 1 were obtained from:

$$V = \dot{B} = \mu \frac{(0.5H)\ A}{t_R(50\%)}$$

where

μ = free space permeability

H = the peak predicted H-field

A = 0.005 m^2 for CML 6A

t_R = the risetime to half peak

The formulation was used because it gave the best average value of the various methods tried. The predicted probe signals do not follow exactly the predicted variation in H-fields at the various probe locations because of small variations in predicted rise time.

Table-1

PREDICTED H-FIELDS

Location	Solid Aluminum Filter				Screen Filter
	With Tank Emission		No Tank Emission		---
	H (A/m)	$V_{\dot{B}}$ (mV)	H (A/m)	$V_{\dot{B}}$ (mV)	H (A/m)
P2	0.80	90	0.72	78	0.92
3	0.84	85	0.75	79	0.95
4	0.67	73	0.56	68	0.71
5	0.36	38	0.31	39	0.39
6	0.12	11	0.10	10	0.12
7	0.67	73	0.56	68	0.71
8	0.67	73	0.56	68	0.71

SECTION II

PIMBS CYLINDER EXPERIMENT

EXPERIMENT DESCRIPTION

The experiment setup consisted of a 90-cm diameter by 90-cm high right circular cylinder, irradiated end on, with a source-to-object spacing of 1.4-m. The axis of the cylinder coincided with the axis of the vacuum tank so that, except for minor disturbances, the experimental configuration was axisymmetric and therefore amenable to accurate solution with the 2D SGEMP codes. The object was suspended by means of nylon lines, as shown if Figure 4a. All surfaces were plated with 60 percent tin, 40 percent lead solder composition by weight.

Instrumentation consisted initially of eight CML-6 $\dot{B}$ probes placed as shown in Figure 4b. The probe at location P8 was damaged before any data were taken, and the probe was removed. Data were transmitted through three microwave data links, which allowed the object to be electrically isolated from the vacuum tank. One of the links (channel 2) had a 6-position switch at its input so that any one of six probes could be switched (by using a dielectric rod) to that channel. The other links were connected directly to a probe (channel 2 to P2) or to terminated cables (channel 1), as shown schematically in Figure 4c. Attenuators were selected and placed in channels 2 and 3 so that the input to the microwave systems were in the system linear range (±26 mV maximum) for predicted signals. The chosen attenuators were 3.16 for channel 2 and 10 for channel 3. In addition, the input balun provided a factor of 2 attenuation in all channels. The transmitter/receiver units (TRU) provided a gain of 20, so that final scale factors are 0.1, 0.316, and 1.0 of scope deflection for channels 1, 2, and 3, respectively.

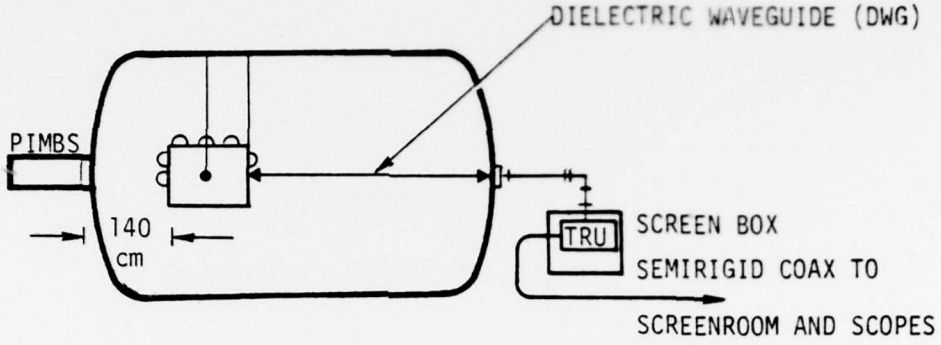

a. General Setup, Side View

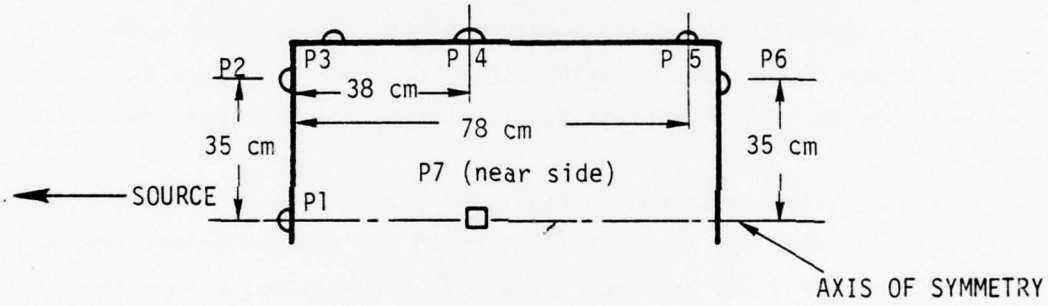

b. Probe Locations

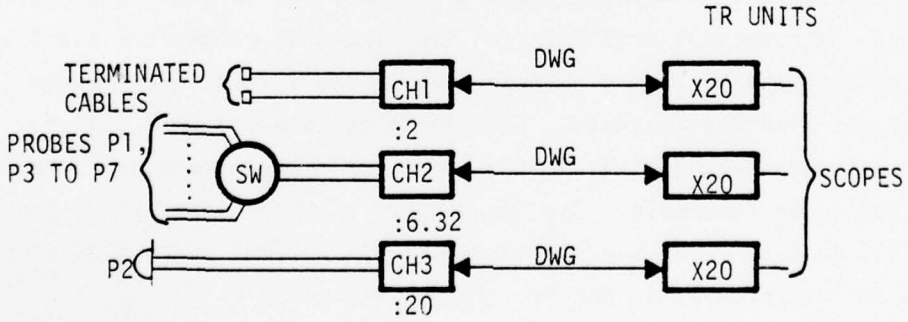

c. Schematic of Instrumentation

Figure 4. Initial test object experiments

An enlarged top view of the tank and object geometry is shown in Figure 5. An overview of the tank, screen box, and screenroom geometry is shown in Figure 6.

The initial photon exposure series, after one day of setup and two days of noise reduction, were made with one additional modification. P4 was direct-wired to a scope through a pair of semirigid coax cables, as shown in Figure 5, so that the body was not isolated from the tank. The second series was made with P4 connected back through the switch so that these cables were removed and the body was electrically isolated. The final series was a repeat of the second series, with a collimator over the source to reduce emission from the wall of the tank by shadowing the wall as much as possible.

Two problems with the instrumentation were encountered during this experiment series. First, one of the $\dot{B}$ probes (P8) was damaged during the initial installation (the connector turned, twisting off the internal connection) and later P5 ceased to give reasonable data (this may be either the probe or the switch). Second, and more troublesome, was gain drift and poor battery life in the microwave data links. The battery life problem is now believed to be due to incorrect charging procedure and should be easily solved. The gain problem has since been worked on by EG&G; but for this experiment, the results have about 15 percent uncertainty due to this drift. As an example of the gain problem, prior to the first data series, the links were calibrated (by their designer, Don Trone) to have a gain of 20. After the test series and after replacing the batteries, two of the systems had nominal gains of 20, but channel 3 (P2) had a gain of 40. Channel 3 was again set to 20, and after the next two test series, a calibration showed that the gain had changed to 17.4 on channel 1 and 22.6 on channel 3, a 13 percent change. Gain drift during vacuum conditions, when calibration was impossible, was also indicated by drift of the RF power level meter on the TRU.

EXPERIMENTAL RESULTS

The results obtained are shown in Figures 7 through 9. The correct scope deflection factors, taking into account the nominal end-to-end microwave system gains, are shown for each data photo. These data are summarized in Table 2, along with PIN diode data. The field data are presented in two formats:

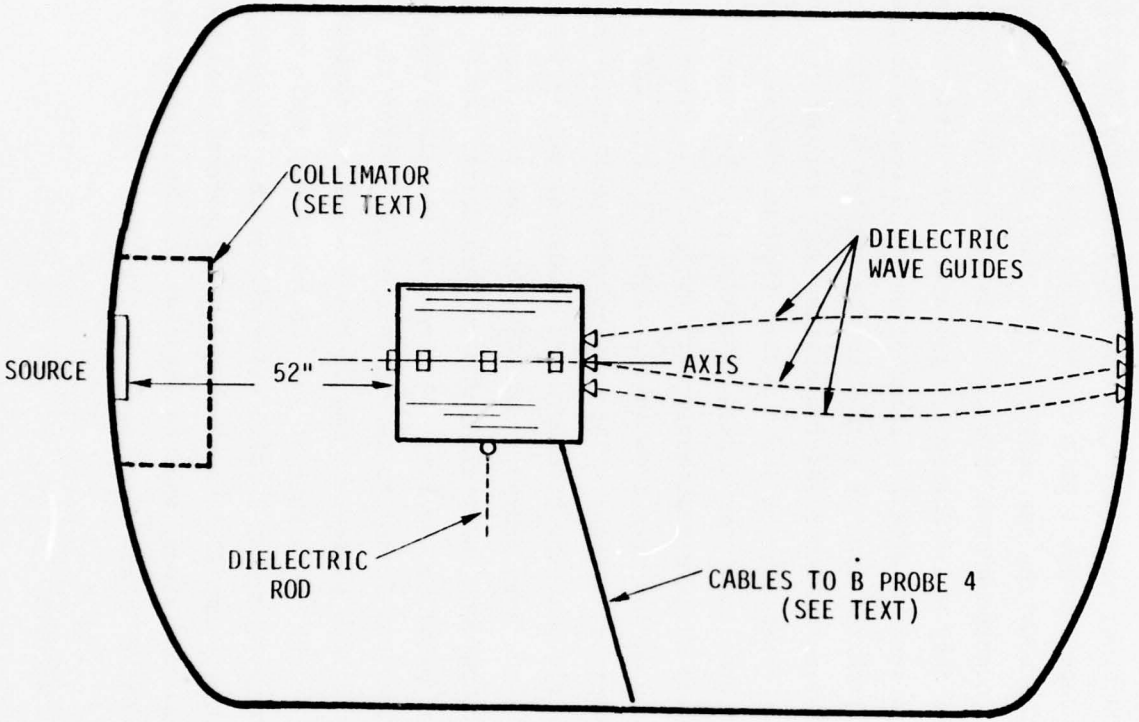

Figure 5. Top view of 0.9 m cylinder in 4 m tank

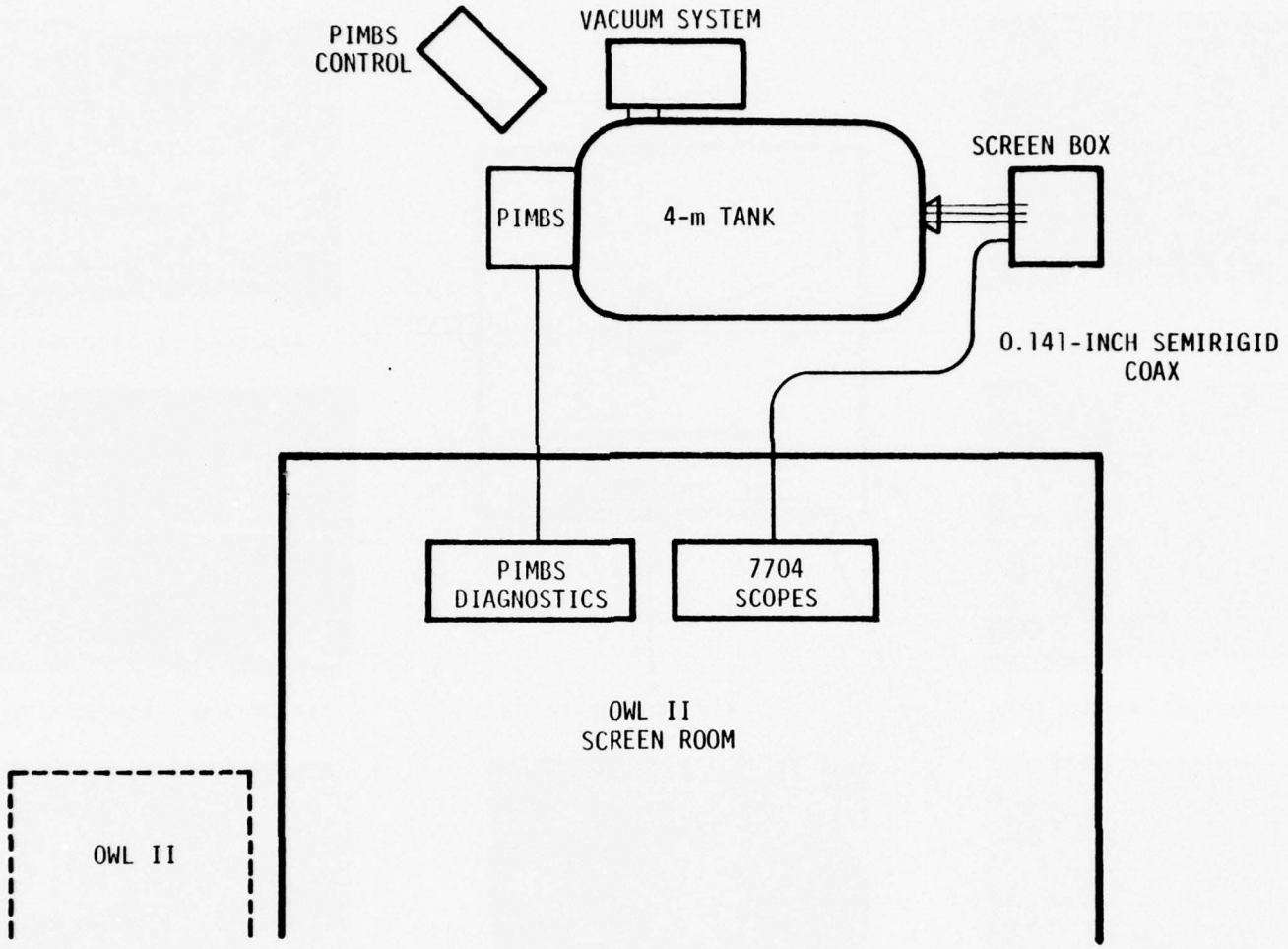

Figure 6. Overview of experimental facility

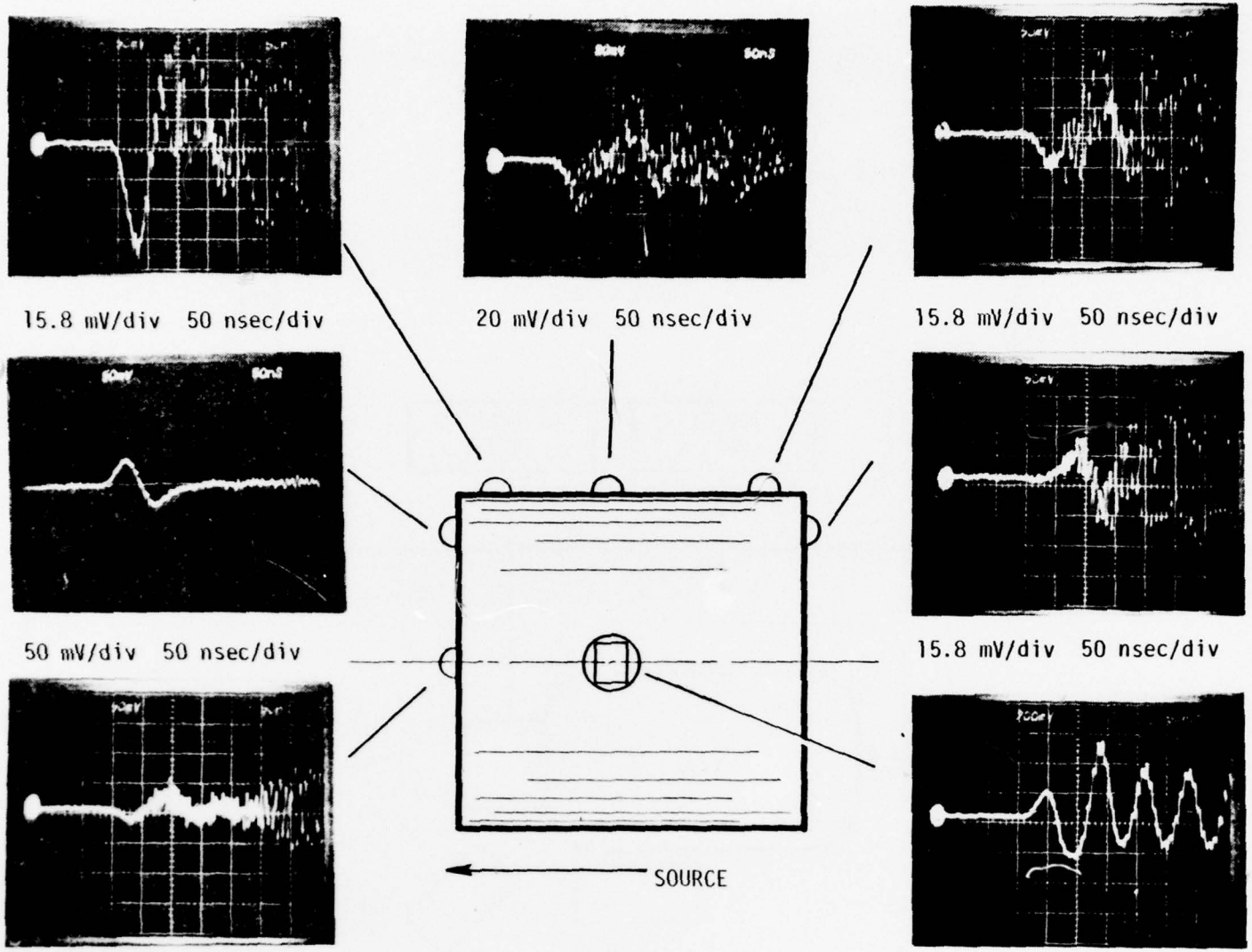

Figure 7. Measured $\dot{B}$ signals with no collimator, body grounded through instrumentation cables

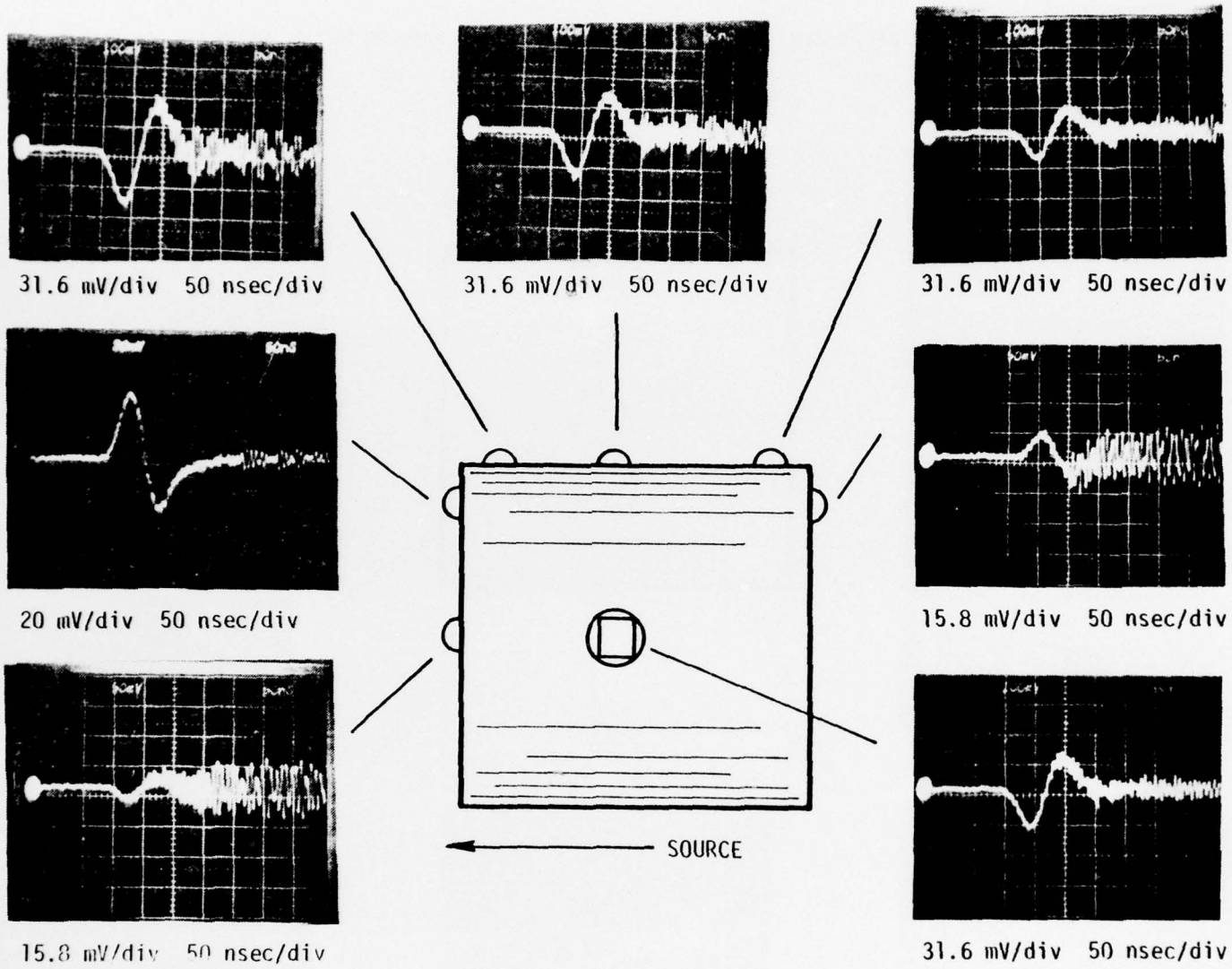

Figure 8. Measured $\dot{B}$ signals with no collimator, isolated body

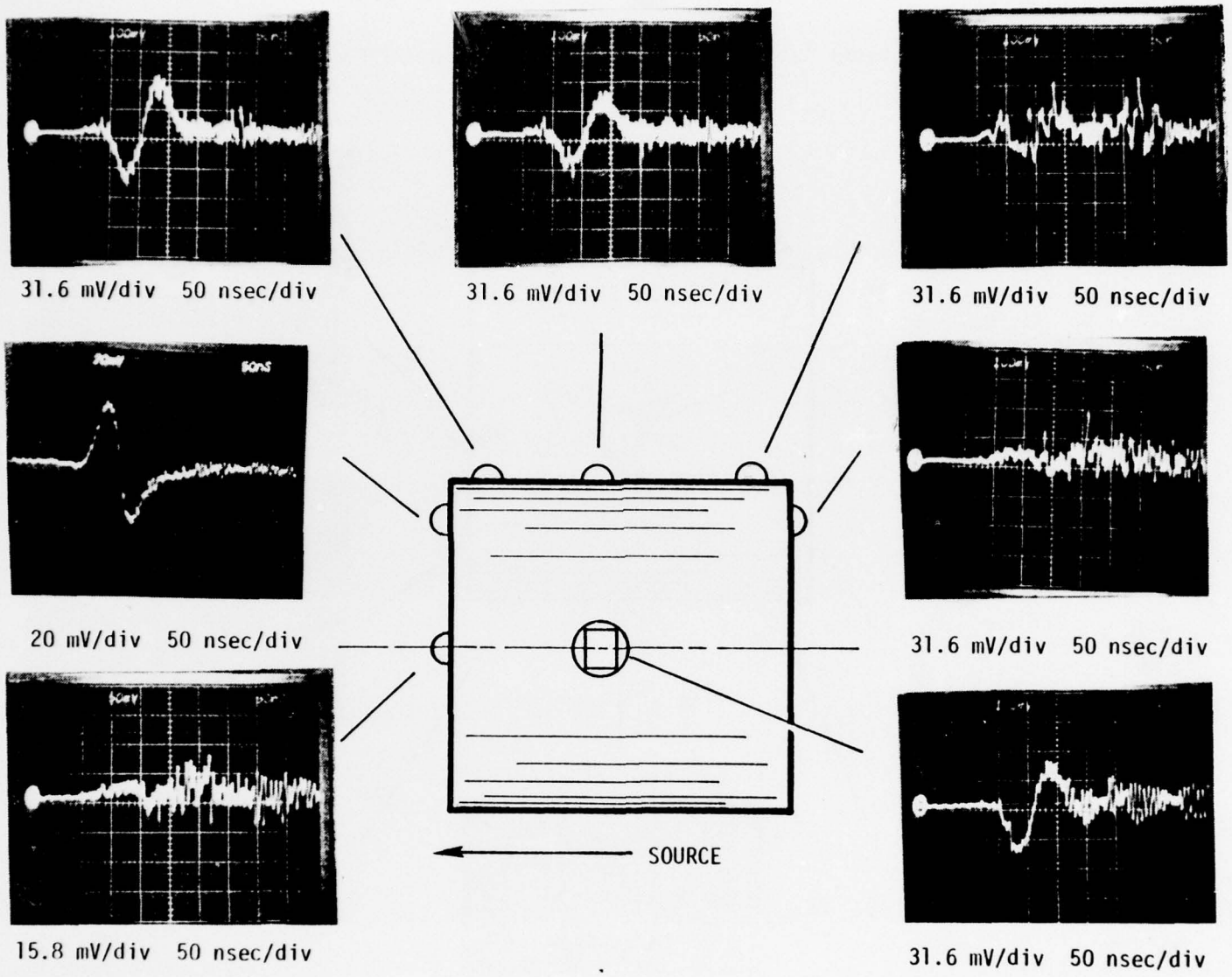

Figure 9. Measured $\dot{B}$ signals with collimator installed, isolated body

(1) the first peak signal value (in mV out of the $\dot{B}$ probe, i.e., all scale factors have been accounted for), and (2) the peak magnetic field. The latter were obtained by graphically integrating the first peak of each waveform, using a planimeter. These data are qualitatively correct, though a better data set needs to be taken on this configuration with reduced noise and more stable microwave system gains. In particular, the data for the grounded body are suspect, as the batteries were dying during the latter half of the series. Considerable difficulty was also encountered in integrating the $\dot{B}$ data because of the large scope deflection factors, which resulted in very small areas under the curves. In all cases, the planimeter integration was checked by assuming a simple triangular shape for each half of the derivative waveform and calculating the approximate area.

The PIN data show the repeatability of each shot from the PIMBS IA pulser, an important consideration, since obtaining a complete set of data required several shots. A typical PIN response is shown in Figure 10a.

The $\dot{B}$ data show considerable noise still remaining even after placing an electromagnetic shield of 1/2 mil of aluminum over the PIMBS converter and wrapping the pulser itself with metal window screen. One channel of the microwave system was used as a background measurement. A photo of the response of this channel is shown in Figure 10b. This channel would measure noise leakage from any possible source except that coupled directly to a $\dot{B}$ probe, since lack of a $\dot{B}$ probe was the only difference between this channel and the active channels. The background channel shows a peak-to-peak noise of the order of only 1 mV or so compared to $\sim$ 30 mV of noise at late times in the $\dot{B}$ data. Thus, it is concluded that the noise in the $\dot{B}$ data is due to noise actually existing in the tank, probably due to leakage through the instrumentation ports. For this experiment, this noise was delayed sufficiently so that good data were obtained in spite of the noise.

The results obtained are reasonable for this experimental configuration. Probe P1 should have a very small (near zero) response, since it is located nominally in the center of the emitting surface. Probes P2 and P3 should have comparable responses, with P2 being slightly smaller; then the responses of P4 through P6 should fall off from the P3 response. Probe P7 should have the same response as P4, since the experiment is basically symmetric. Thus,

Figure 10a. Typical PIN response

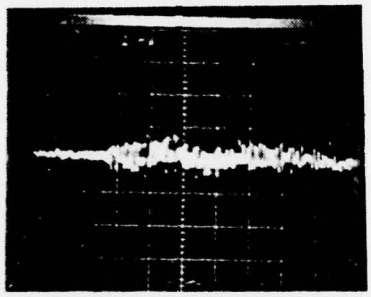

Figure 10b. Noise measurement on instrumentation system background channel

the relative responses measured are reasonable. From the standpoint of absolute amplitude, the approximate field at P3 can be calculated from:

$$H = \frac{I_E}{2\pi r} = \frac{\left(\frac{2.2}{1.4}\right)^2 (0.8\ A/m^2)\ (0.636\ m^2)}{2\pi\ (0.45)}$$

$$= 0.44\ A/m$$

where 0.8 A/m^2 is the measured emission current density for the biased diode at 0 bias, 0.636 m^2 is the area of the emitting face of the object, and the $(2.2/1.4)^2$ factor accounts for the difference in location of the object and the biased diode (which was 2.2 m from the source). The integrated B response of P3 is about 20 percent lower than the H field estimated by this simple calculation.

SECTION III

PREDICTION-EXPERIMENT COMPARISON

The ABORC predictions are in the form of H fields, while the experimental results are in the form of $\dot{B}$ measurements; therefore, direct comparisons are not possible. The small size of the measured $\dot{B}$ responses makes integration to obtain H fields difficult, especially with the planimeter technique previously used to obtain the results shown in Table 2. The measured data for point P2, near the top edge of the cylinder, for the configuration without a collimator, which is the most symmetric and which can therefore be most accurately modeled with ABORC, has been carefully digitized at 10 nsec intervals and integrated to obtain the results shown in Figure 11. Note that the integrated $\dot{B}$ signals should be proportional to the magnetic flux linking the sensors at time t, which should approach zero for large times. The accuracy of these integrations is suggested by the residual errors, which are shown at the 250 nsec time for each probe location. All of the larger signals had cummulative errors of 11 percent or less except for P7, which had 26 percent. Probe P6, which is a small signal, had a cummulative error of about 50 percent. The error band for the peak value of each of these is expected to be even smaller, since the failure to integrate back to zero results generally from the late time noise, which made digitization of the latter portions of the signals more uncertain. The peak values, 10 to 90 percent risetimes, and pulse widths at half maximum for the predicted and measured H fields are compared in Table 3, along with the ratio of predicted and measured peak H fields. There is a definite pattern to this ratio, with agreement tending to be worse on the emitting surface and slowly improving toward the far end of the object. Stated another way, the predictions tend to fall off more rapidly than the measured signals.

The predictions are higher by $2.5\ ^{+0.6}_{-0.7}$ than the measured fields, and the questions naturally arise as to why the agreement is not better. The most likely

reason appears to be possible difference between the emission current used in the ABORC predictions and the actual emission current. In fact, there is even considerable room for discussion about just what the actual emission

Table 2

EXPERIMENTAL RESULTS FOR CYLINDER

	Isolated Body				Grounded Body	
	No Collimator		Collimator		No Collimator	
Probe	Voltage mV	H* A/m	Voltage mV	H* A/m	Voltage mV	H* A/m
P1	6	0.066[1]	5	---	6	---
P2	42	0.32	40	0.32	40[2]	---
P3	54	0.36	50	0.35	54	---
P4	44	0.26	34	0.23	26	---
P5	26	0.20	--	---	18	---
P6	11	0.10	9	0.050	12	---
P7	38	0.26	48	0.50	48[3]	---
P8	--	---	--	---	--	---
PIN	4.4 to 4.6 units		3.7 to 3.9 units[4]		4.4 to 4.5 units	

NOTES:

* Obtained by planimeter integration of $\dot{B}$ signals

1 Sensor failed, no data

2 Except for one shot of 64 mV

3 Data doubtful. This probe responds to ringing currents flowing on the hardwire. Subsequent peaks reached 150 mV and ringing persisted for hundreds of nsec

4 Lower PIN response due to shadowing by collimator

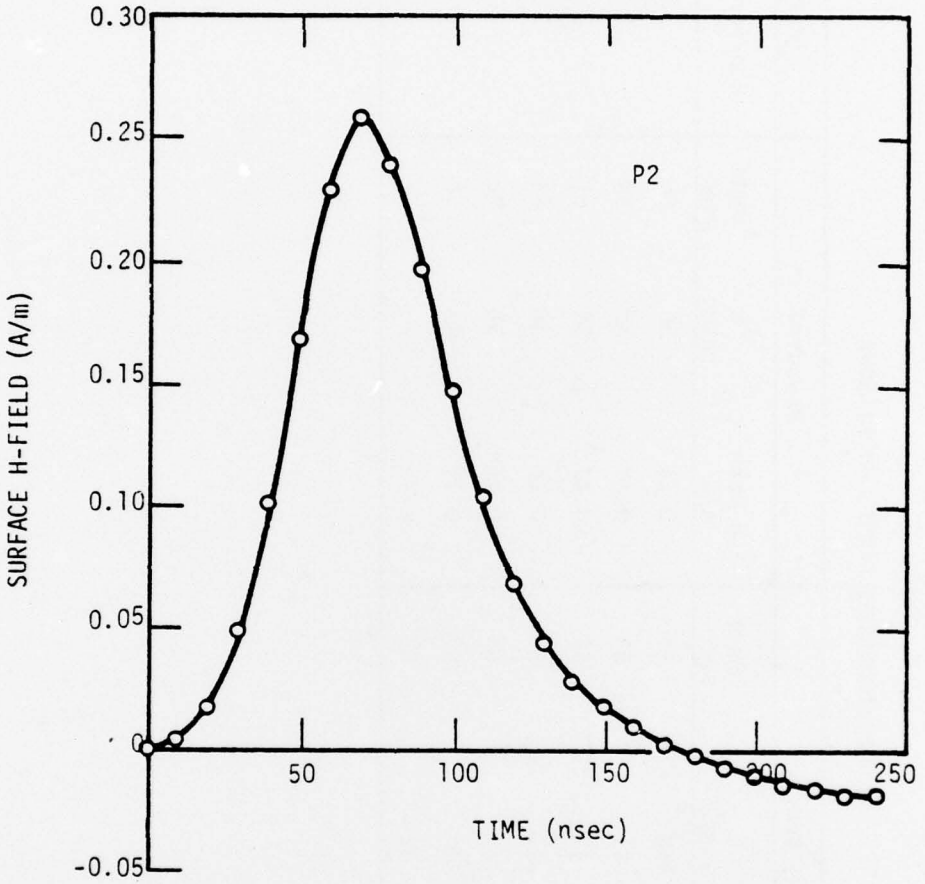

Figure 11. Measured H fields resulting from integration of $\dot{B}$ signals

Table 3

PREDICTION/EXPERIMENT COMPARISONS

Probe	Predicted			Measured			Ratio
	H Peak A/m	t_R nsec	t_{FWHM} nsec	H Peak A/m	t_R nsec	t_{FWHM} nsec	H pred/ H meas
2	0.80	36	58	0.26	36	60	3.1
3	0.84	41	58	0.32	38	59	2.6
4	0.67	42	57	0.27	38	61	2.5
5	0.36	41	56	0.16	36	63	2.3
6	0.12	47	63	0.068	38	72	1.8
7	0.67	42	57	0.27	41	68	2.5
8	0.67	42	57	----	--	--	---

current should be, since total emission from the body itself was not measured. The measured current density from the biased diode experiment is shown in Figure 12 as a function of grid bias. The diode was at 2.2 m from the source, ~45 degrees off axis, while the cylinder was at 1.4 m, on axis. Taking into account the $1/r^2 \cos\theta$ variation, which most closely approximates the results of the dosimeter mapping experiment, the emission current density at the cylinder surface would then be as shown in Figure 13. The most obvious result from this calculation is that the current emitted from the object is <u>at most</u> 2.8 amps, and probably less, rather than the 3.5 amps used in the ABORC predictions. Thus, the predictions are high, due at least partially to using too high an emission current in the predictions. If the actual emitted current is the 0 bias current of 1.8 A, the prediction would be high by a factor of 2 as a result, and this would explain most of the difference between the predicted and measured signals.

There is an independent justification for this lower emission current. On a later experiment, with a slightly different filter over the source, a TLD stack was placed 41 inches from the filter and measured a fluence of 1.2×10^{-5} cal/cm^2. Scaling the fluence to the actual location of 52 inches from the filter (adding about 2 inches between the source and filter) results in a measured fluence of 7.6×10^{-6} cal/cm^2 at the emitting surface of the object, rather than the predicted 1.4×10^{-5} cal/cm^2. For the 2×10^{-6} coul/cal emission predicted by QUICKE2 and a 55 nsec pulse width, the body emission current is then calculated to be

$$I_E = \frac{(7.6 \times 10^{-6} \text{ cal/cm}^2)\ (2 \times 10^{-6} \text{ coul/cal})}{55 \times 10^{-9} \text{ sec}} (6360 \text{ cm}^2)$$

$$= 1.76 \text{ amperes},$$

which is in excellent agreement with the 0 bias diode results also scaled to the object location. The difference in filters is a high-transparency screen plus 1/4 mil of mylar for the TLD measurement instead of the 1/2 mil of aluminum used for the cylinder exposures. This would have only a slight effect on the fluence reaching the object; therefore, it appears that the fluence was lower than expected by almost a factor of 2.

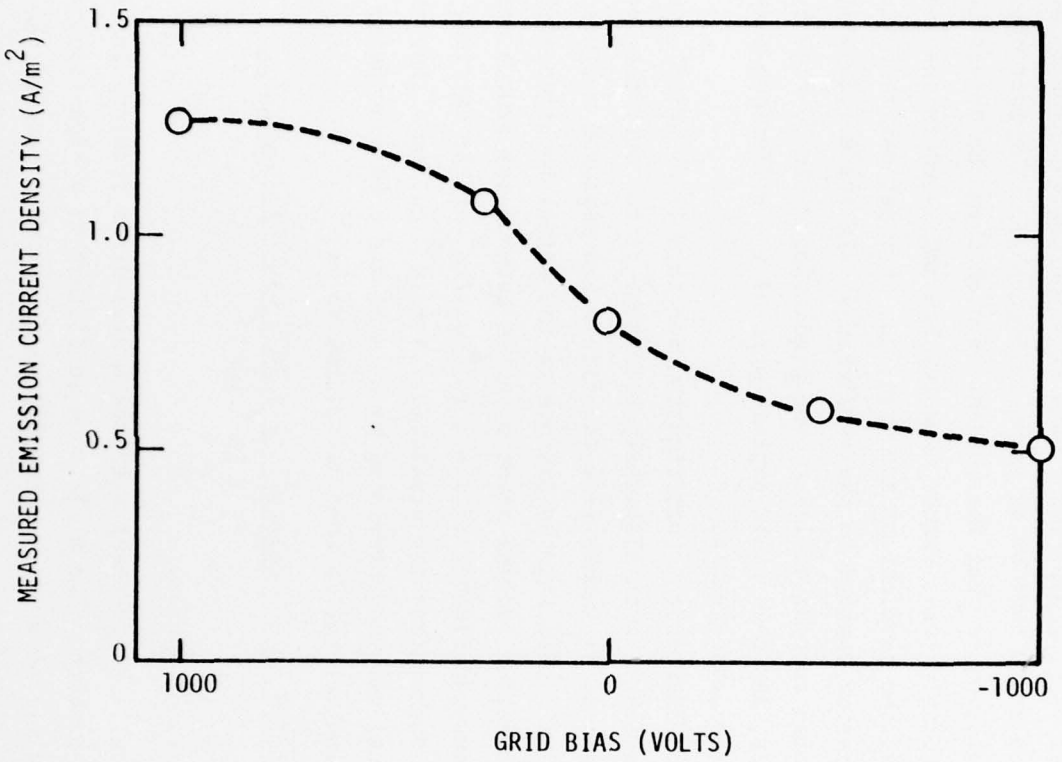

Figure 12. Measured reverse emission current density from solder as a function of grid bias

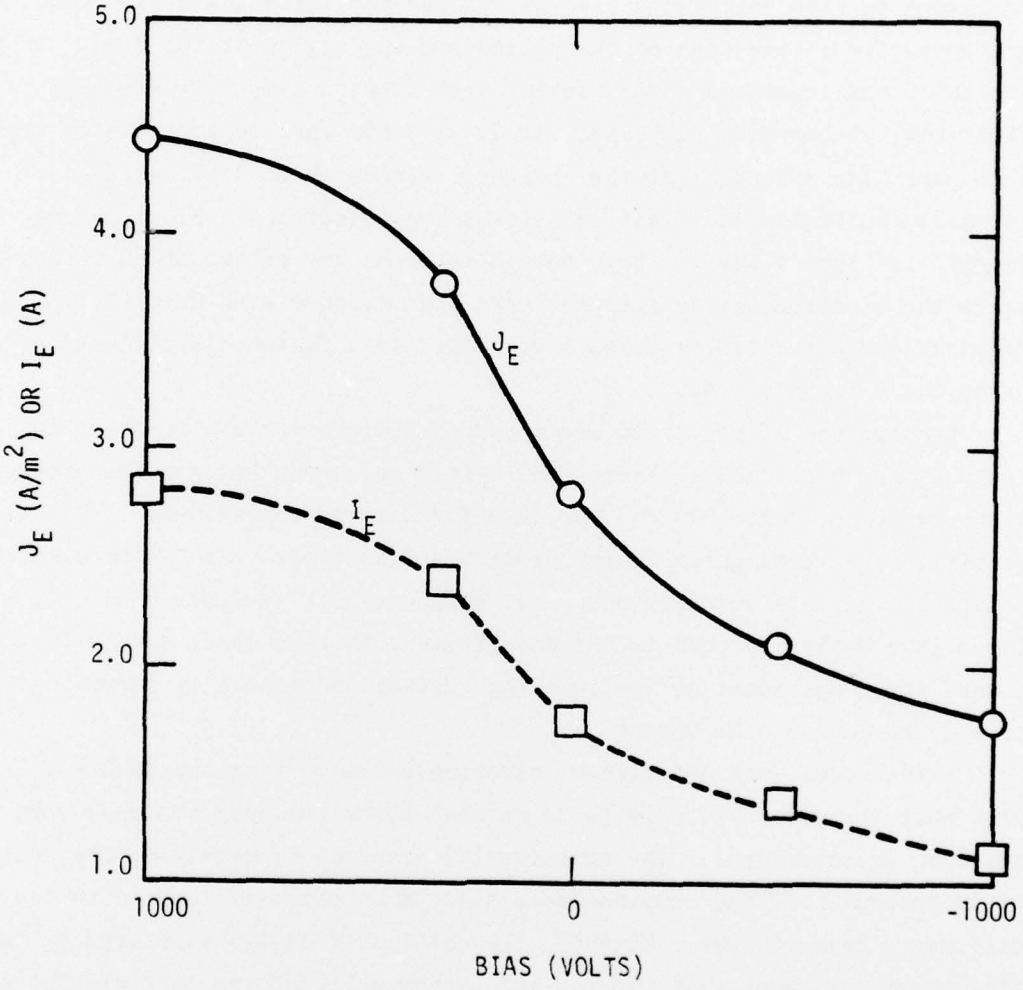

Figure 13. J_E and I_E from cylinder surface as a function of bias

The issue in doubt is whether the emission current should be the 0 bias current, the forward bias current, or something in between. Best agreement between predicted and measured cylinder responses clearly occurs for the 0 bias current value, and one is tempted to simply say that this justifies using this current. But the questions of why the diode current continues to rise as forward bias is applied and where these same conditions are operative in the case of the cylinder keep nagging at the mind. If the source of the increased diode current with forward bias is low-energy electrons, as has been suggested, it is probably most appropriate to leave them out. The potential of the cylinder reaches about 2 kV, which is certainly sufficient to limit such low-energy electrons. Electrons of energy less than 1 keV are also not included in any of the ABORC predictions, since the electron energy spectrum used was obtained with QUICKE2, which does not predict emission below 1 kV. This is a further justification for using the 0 bias current.

Comparisons of predicted and measured $\dot{B}$ signals are also shown in Table 4, for both cases. These show better agreement between the predictions and experiment than was the case for H-field comparisons. This is partially due to slightly longer predicted rise times than the integrated $\dot{B}$ signals indicate actually occurred, which results in lower predicted $\dot{B}$. There is a weaker pattern to the disagreement in this case, with a tendency toward worse agreement at the emitting surface and generally improving toward the back of the object.

Predictions with and without electron emission from the tank wall show that the effect is a 10 to 20 percent lower cylinder response when this emission is suppressed. The experimental accuracy is barely of the order of 20 percent, but the response does tend to be slightly lower with the collimator than without. However, the collimator design (dictated by the line source) is such that the top and bottom walls of the tank will be well shadowed but the sides will not be. This is evidenced by the fact that the PIN response is from 4.4 to 4.6 divisions for a number of shots without the collimator and drops to only 3.7 to 3.9 divisions with the collimator. That is, the collimator shades only a portion of the source area from the side wall where the PINs are located.

Table 4

COMPARISON OF MEASURED AND PREDICTED PEAK B PROBE SIGNALS

Probe	No Collimator Pred/Exp	Collimator Pred/Exp
2	2.14	1.95
3	1.57	1.58
4	1.66	2.0
5	1.46	---
6	1.00	1.11
7	1.92	1.42
Average	1.63	1.61

SECTION IV

SUMMARY AND CONCLUSIONS

The analytical H-field predictions for this experiment are a factor of $2.5\ ^{+0.6}_{-0.7}$ higher than the experimental results, with an uncertainty of less than 10 percent in the integrated $\dot{B}$ results. The emission current used in the predictions (3.5 amps) is higher by a factor of 1.25 than the absolute maximum (forward biased) emission current which can be estimated for the object, based on the biased diode experiment results, and a factor of 2.0 higher than the 0 bias emission current. Thus, the disagreement is partially explained by a discrepancy between the actual emission current and that used in the analysis. The 0 bias current is considered most reasonable for reasons discussed in the comparisons, and it is concluded that the predictions range from 54 percent high at the emitting surface to 12 percent low at the back end of the object. The experimental accuracy is believed to be of the order of 15 percent.

One obvious problem that has not yet been resolved is the proper characterization of the emission electron spectrum and yield. While for a system-level SGEMP analysis the factor of 2 uncertainty estimated here may not be too important by itself, a few such factors of 2 could result in an expensive and unnecessary hardening approach.

Careful electron emission experiments should be done to resolve this issue. The authors feel that prediction accuracy of better than 10 percent should be achievable for the simple geometry treated here, if the emission is accurately characterized.